Reformulation of solar cell physics to facilitate experimental separation of recombination pathways

Sachit Grover, Jian V. Li, David L. Young, Paul Stradins, and Howard M. Branz
National Renewable Energy Lab, Golden, Colorado 80401, USA

Experimentally identifying the spatial distribution of recombination in a solar cell is challenging, with only semi-quantitative information available from conventional characterization techniques. We develop a formulation of solar cell physics, based upon well-justified analytic approximations, to quantitatively extract information about recombination in different cell regions. We derive the dependence of V_{OC} on light-intensity, temperature, and strength of recombination in the space-charge, quasi-neutral, and interface regions. Expanding the scope and utility of commonly used characterization techniques, we apply this formulation to evaluate the spatial distribution of recombination in exemplary crystalline silicon heterojunction and polycrystalline Cu(In,Ga)Se$_2$ solar cells. © 2013 AIP Publishing LLC. [http://dx.doi.org/10.1063/1.4819728]

Conceptually, it is well understood that the distribution of photocarrier recombination among the regions of a solar cell is governed by the distribution of defects, electric field, and charge carriers.[1] The Shockley-Read-Hall (SRH) statistics provide the mathematical framework for calculating the rate of recombination through defect states.[1,2] SRH recombination may occur in the quasi-neutral region (QNR), the space-charge (depletion) region (SCR), at interfaces, and at surfaces. The first three of these regions are marked in Fig. 1 and are the focus of this work. We overcome the limitations of existing analysis techniques in providing quantitative separation of recombination in different regions of a solar cell through a framework that leverages existing V_{OC} measurements. Accurate distinction and identification of the recombination channels can help focus efforts to improve material quality and device fabrication upon the most important physical regions of a solar cell under development.

The dark current-voltage [$J(V)$] curve normally serves as a first diagnosis of recombination in a solar cell. At low forward bias, recombination is assumed to be primarily in the SCR, which leads to an ideality factor (n) of 2. Recombination in the QNR increases at high forward bias as the minority carrier concentration rises, leading to $n = 1$. A two-diode model combining these two recombination mechanisms can then be used to fit the $J(V)$ curve.[2] The resulting magnitudes of the saturation current densities (J_{01}, J_{02}) are often used as a relative measure of QNR and SCR recombination, respectively. However, in heterojunctions such as Cu(In,Ga)Se$_2$ (CIGS) or a-Si/c-Si solar cells, this simple approach is confounded by recombination at interfaces, which also contributes to $n = 1$ recombination.[3] This necessitates measurements such as voltage bias quantum efficiency and temperature-dependent open-circuit voltage ($V_{OC}(T)$) to check for recombination in the SCR and at junction interfaces.[4] These techniques provide only *qualitative* information regarding the distribution of recombination among the different regions of a heterojunction solar cell. Another common approach used to model diodes is to combine the $n = 1$ and $n = 2$ terms to get an effective ideality factor n_e.[4,5] Beyond providing a crude sense of the distribution between SCR and

QNR recombination in the cell, n_e offers little physical insight. Moreover, the actual slope of the $J(V)$ curve changes with bias,[4] and assuming a constant slope leads to loss of meaningful information.

In this letter, we utilize the exact balance between generation and recombination rates at V_{OC} to derive a set of analytic approximations relating recombination in various regions of a solar cell to easily measured quantities. By tracking the light-intensity dependence of V_{OC}, and implicitly following the excess carrier concentration, we study the spatially changing dynamics of carrier recombination. We also relate our analysis to the conventional two-diode model. Instead of analyzing the slope and intercept in different segments of the $J(V)$ curve, we combine the $n = 1$ and $n = 2$ recombination mechanisms into a single common equation for V_{OC}. While our approach could have been applied equally well to any point on the $J(V)$ curve, we choose to analyze the easily measured light-intensity (suns-V_{OC}) and temperature dependences of V_{OC}. This approach provides two key benefits: (1) we focus on V_{OC}, which is the voltage of maximum
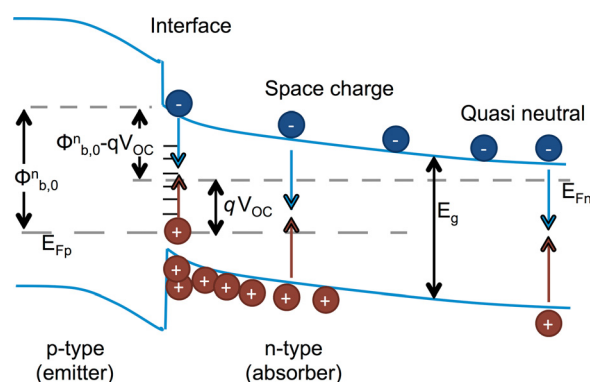

FIG. 1. Schematic band diagram of a type-I heterojunction solar cell with an n-base under illumination, in open-circuit bias. E_g labels the bandgap, E_{Fp} and E_{Fn} label the hole and electron QFL, and $\phi^n_{b,0}$ is equal to the barrier height at zero bias (here, illustrated under light-bias). The separation between the absorber conduction-band and majority QFL at the interface ($\phi^n_{b,0}$–qV_{OC}) determines the majority carrier concentration through the Boltzmann factor.

recombination in a solar cell (all light-generated carriers recombine), and (2) we remove the effect of series resistance and S-curves that would otherwise confound the analysis of $J(V)$ curves. There are differences in Fermi statistics governing the different recombination mechanisms; by assigning physical meaning to the extrapolated value of $V_{OC}(T)$ at $0\,K$, these differences enable us to separate the contributions of various recombination mechanisms. Our comprehensive analytical framework provides a meaningful interpretation of the commonly measured $suns-V_{OC}$ and $V_{OC}(T)$ data and unifies these measurements to enable quantitative evaluation of recombination in different regions of a solar cell.

The statistics of SRH recombination depend on the local charge carrier concentrations in a semiconductor and the characteristics of the defects through which carriers recombine.[6] We divide the solar cell into three regions of carrier concentration (QNR, SCR, and interface) and write the recombination rate in each region. For simplicity, emitter and surface recombination are omitted here, but they could easily be included in our framework. We simplify the equations for recombination rate by expressing the carrier concentrations in different regions of the solar cell in terms of a common variable β. Finally we equate the electron-hole pair generation in the cell to the total recombination and obtain an analytic dependence for V_{OC} on recombination parameters and operating conditions.

The V_{OC} of a solar cell under illumination is equal to the electron and hole quasi-Fermi level (QFL) separation at the contacts. In the absence of current flow, the QFL separation remains constant across the width of a cell.[8] The QFL separation at any point in a diode is logarithmically related to the product of electron and hole concentrations ($n_e p_h$). A spatially independent QFL separation leads to a constant $n_e p_h$ product that we leverage by defining a spatially independent variable $\beta = (n_e p_h / n_i^2)^{1/2}$; where n_e, p_h, and n_i refer to the electron, hole, and intrinsic carrier concentrations, respectively. We can express V_{OC} in terms of β as[2]

$$V_{OC} = E_{Fn} - E_{Fp} \frac{kT}{q} \ln\left(\frac{n_e p_h}{n_i^2}\right) = \frac{kT}{q} \ln(\beta^2), \quad (1)$$

where q is the electronic charge and k is the Boltzmann constant. Therefore, the carrier concentrations at any location are embodied in beta, through the measured V_{OC}.

The general form of SRH recombination rate per unit volume (U_{SRH}) is given by[2]

$$U_{SRH} = \frac{n_e p_h - n_i^2}{\tau_p(n_e + n_1) + \tau_n(p_h + p_1)}. \quad (2)$$

The τ_p and τ_n are time constants related to the trap density (N_t) and capture cross-section for holes (σ_p) and electrons (σ_n) as $\tau_p = (N_t \sigma_p v_{th})^{-1}$ and $\tau_n = (N_t \sigma_n v_{th})^{-1}$. The v_{th} refers to the usual average thermal velocity of charge carriers. The denominator in Eq. (2) also contains two factors n_1 and p_1 that signify the electron and hole occupancy of the defect level. We assume that the most effective recombination centers are located close to the middle of the energy gap, and adopt the common assumption that n_1 and p_1 are negligible compared to the excess carrier concentration or the doping density.

In the SCR or depletion region of the solar cell, the electron and hole concentrations each vary monotonically with position but decay in opposite directions from maxima at either end of the SCR. Maximum recombination in the depletion region, U^d_{SRH}, occurs at the point of equal electron and hole concentrations, and we denote the concentrations at this location as n_m and p_m, respectively. Following Sze,[2] Eq. (2) can be simplified at the point of maximum recombination and multiplied by the depletion width (W_d) to approximate the rate of total recombination per unit cell area in the depletion region, as

$$R^d = W_d U^d_{SRH} = \left(\frac{W_d n_i}{\tau_p + \tau_n}\right)\beta = R_0^d \beta, \quad (3)$$

where $\beta n_i = n_m = p_m \gg n_i$ at the point of maximum recombination in the depletion region. We note that the product $n_m p_m = n_e p_h$. Although Eq. (3) slightly overestimates the recombination in the depletion region,[7] it provides the correct β dependence for R^d and suffices for this derivation. Neglecting the weak light-intensity dependence of W_d, we use R_0^d to denote the strength of depletion recombination independent of bias conditions. The light-bias dependence of recombination is contained in β.

In the QNR or the base of the solar cell, denoted by b, the total recombination per unit area can be expressed as

$$R^b = W_b U^b_{SRH} = W_b \frac{\Delta p}{\tau_p} = \left(\frac{W_b n_i^2}{N_D \tau_p}\right)\beta^2 = R_0^b \beta^2, \quad (4)$$

where Δp represents the excess minority carrier concentration and W_b is the width of the quasi-neutral region or the bulk. Here, we make use of the equality $N_D \Delta p / n_i^2 = \beta^2$ in the QNR at V_{OC}. Though, we have simply written Eq. (4) for n-base cells here, an analogous equation holds for p-base cells. We also assume low-level injection ($N_D \gg \Delta p$) such that recombination rate in the QNR of the n-type absorber in Fig. 1 is limited by the availability of minority carriers that recombine with a lifetime τ_p.

Interface recombination in a one-sided heterojunction is generally limited by the availability of majority carriers[3] as a large number of minority carriers are available due to the proximity of the QFL to the minority-carrier band. Such a situation is depicted in Fig. 1 for an n-type absorber, where the proximity of the hole QFL to the valence band leads to an inversion layer at the interface. The recombination-limited electron concentration at the interface is set by the Boltzmann approximation of electrons referenced to the electron QFL, $n_e = N_C \exp\{-(\phi^n_{b,0} - qV_{OC})/kT\}$. Recombination rate at the interface is generally expressed in terms of S_n, the surface recombination velocity.[3] The total SRH recombination per unit area at the interface is then given by

$$R^I = S_n n_e = S_n N_C \exp\left\{-\frac{\phi^n_{b,0}}{kT}\right\}\beta^2 = R_0^I \beta^2. \quad (5)$$

The V_{OC} dependence of R^I is contained in β^2, through Eq. (2). The bias-independent strength of interface recombination (R_I) is given by R_0^I.

We define an average generation rate (G_{avg}) as the total generation rate in the cell divided by the total cell thickness

(W). G_{avg} has the units of cm^{-3} s^{-1} or sun/cm since solar photon-flux is measured in suns or cm^{-2} s^{-1}. Equating the overall SRH recombination per unit area in the cell given by the sum of Eqs. (3)–(5), to the total generation ($\Sigma R = G_{avg}W$) we obtain a quadratic equation in β as

$$[R_0^I + R_0^b]\beta^2 + R_0^d\beta = \int_W G_x dx = G_{avg}W, \qquad (6)$$

which is the master equation for recombination in the solar cell. Note that the units of R_0^d, R_0^I, and R_0^b are cm^{-2}s^{-1}. Solving for β in terms of R_0^d, R_0^I, and R_0^b, and then using Eq. (1) to find V_{OC} in terms of β, we obtain

$$V_{OC} = 2\frac{kT}{q}\ln[k_1(\sqrt{1 + k_2 G_{avg}} - 1)], \qquad (7a)$$

$$\text{where}\quad k_1 = \frac{R_0^d}{2(R_0^I + R_0^b)}; \quad k_2 = 4W\frac{(R_0^I + R_0^b)}{(R_0^d)^2}. \qquad (7b)$$

Equations (7a) and (7b), together, give the combined dependence of V_{OC} on SRH recombination in the three regions. The temperature dependence of V_{OC} is also contained in this equation, explicitly in kT and implicitly in n_i, k_1, and k_2. Eq. (7) also gives the V_{OC} dependence on light intensity (via G_{avg}) from which we will derive an expression for the ideality factor; the factor of 2 outside the logarithm does not imply that the ideality factor of the diode is 2.

By analogy to the conventional ideality factor,[2] we define a bias-dependent differential ideality factor as

$$n = \left[\frac{kT}{q}\frac{d\left(\ln(G_{avg})\right)}{dV_{OC}}\right]^{-1} \qquad (8)$$

that leads from Eq. (7a) to

$$n(G_{avg}) = \frac{k_2 G_{avg}}{\sqrt{1 + k_2 G_{avg}}[\sqrt{1 + k_2 G_{avg}} - 1]}. \qquad (9)$$

As with V_{OC} in Eq. (7a), we have brought out the explicit dependence of n on G_{avg} in Eq. (9), while the dependences on recombination mechanism and temperature are embedded in k_2.

In Eqs. (7a) and (9), we have related easily measured quantities, V_{OC} and n, to parameters governing the rates of recombination in the different regions of the cell. The light-intensity and temperature dependence of these observables enable quantitative estimates of the recombination parameters. Later in this letter, we explicitly calculate the temperature dependence of V_{OC} and provide an example using $V_{OC}(T)$ to quantify interface recombination. Next, however, we describe the details of a simple procedure, based only on measured $V_{OC}(G_{avg})$ data, for separating QNR and SCR recombination; our example is a silicon heterojunction solar cell with negligible interface recombination.

As a first analysis step, we determine the relative strength of $n = 1$ and $n = 2$ recombination mechanisms by fitting $n(G_{avg})$ from Eq. (9) to experimental data, and thereby obtain k_2. Knowing k_2, we then fit experimental data for
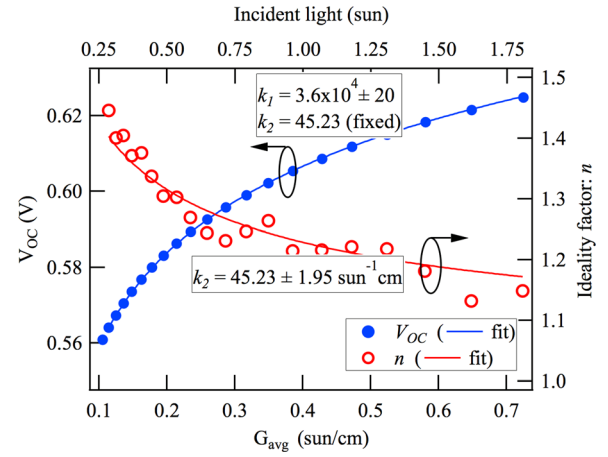

FIG. 2. Open circuit voltage (V_{OC}) and ideality factor (n) as a function of generation rate (G_{avg}) for a Si heterojunction solar cell measured using suns-V_{OC}. The sub-μs lifetime of the absorber implies steady-state condition at each light intensity. The curves (solid lines) are fits to experimental data (circles), which yield the values of k_1 and k_2.

$V_{OC}(G_{avg})$ to Eq. (7a) and obtain k_1. Knowing k_1 and k_2, we can calculate the relative strength of $n = 1$ and $n = 2$ recombination mechanisms using Eqs. (2) and (4). If there is no significant interface recombination, k_1 and k_2 are sufficient to quantify the distribution of recombination in the SCR (R^d) and QNR (R^b) through the parameters R_0^d and R_0^b.

In Fig. 2, we plot the V_{OC} and the n, we obtain from suns-V_{OC} data using Eq. (8) for a heterojunction solar cell made on an epitaxial silicon absorber.[9,10] The data are measured using a Sinton Instruments WCT-100 photoconductance tool.[11] In previous work on these homoepitaxial absorbers, we reported that the extrapolation of $V_{OC}(T)$ to 0 K gives an E_a close to the bandgap of silicon, which indicates negligible interface recombination.[12] Therefore, in the present analysis, we assume that the interface recombination is small and focus on the problem of separating recombination rates in the SCR and QNR. In order to apply Eq. (8) for calculating n from V_{OC}, we use a constant scaling-factor to convert the measured light intensity to G_{avg}. As a scaling-factor, we use the ratio of the 1-sun J_{SC} to the current density available from the solar-spectrum above the bandgap of the absorber. This assumes that all the photogenerated carriers are collected with 100% efficiency at J_{SC}, independent of the light intensity. Since we analyze a very thin c-Si absorber, the optical loss is significant $\sim$60%.

By applying Eqs. (7a) and (9) to fit the light-intensity dependence of V_{OC} and n, we obtain $k_2 = 45$ sun^{-1}cm or 6.4×10^{-20} cm^{3}s and $k_1 = 3.6 \times 10^4$. In the absence of interface recombination, we use these values to calculate the recombination in the SCR and QNR. We equate the product $k_1 k_2$ from Eq. (7b) to the values obtained from fitting and knowing the cell width ($W = 4\,\mu$m), we find $R_0^d = 3.5 \times 10^{11}$ cm^{-2}s^{-1} and $R_0^b = 5 \times 10^6$ cm^{-2}s^{-1}. At the measured 1-sun V_{OC} of 620 mV, we apply Eq. (1) to calculate $\beta = 1.65 \times 10^5$ cm^{-3}. Substituting R_0^d, R_0^b, and β in Eqs. (3) and (4), we estimate that at 1-sun illumination, nearly 30% of the total recombination occurs in the SCR and the remaining 70% occurs in the QNR. Assuming $\tau_p = \tau_n$ in Eqs. (3) and (4), we then calculate the width of the depletion region to be

$W_d = 35\,\text{nm}$ and the bulk lifetime to be $\tau_p = 80\,\text{ns}$ at 1-sun illumination and open-circuit.

In the limit of small and large $k_2 G_{avg}$, the ideality factor in Eq. (9) simplifies as

$$n\{k_2 G_{avg} \to 0\} = 2, \quad n\{k_2 G_{avg} \to \infty\} = 1, \qquad (10)$$

respectively, implying that SCR recombination dominates if $k_2 G_{avg}$ is small, and QNR and/or interface recombination dominate if $k_2 G_{avg}$ is large. In epitaxial Si cells with higher concentration of defects, we observe k_2 to be much smaller than in this high-quality cell, indicating that the fraction of recombination in the SCR increases with increasing concentration of defects.

As the second analysis step, we separate the $n = 1$ recombination mechanisms (i.e., interface and QNR) by comparing the zero-Kelvin extrapolation of the measured $V_{OC}(T)$ data to its analytical dependence on the interface barrier height ($\phi^n_{b,0}$) and the absorber bandgap (E_g). Linear extrapolation of qV_{OC} to 0 K provides an activation energy, E_a. By calculating k_1, k_2, and E_a from the measured light and temperature dependence of V_{OC}, one can then calculate the individual strengths of all three recombination mechanisms. We next show the details of this analysis and then apply it to study a series of CIGS solar cells.

We derive the required equations by simplifying Eq. (7a) in the limit of $k_2 G_{avg} \gg 1$. Experimentally, this limit is obtained at high light intensities that lead to a near unity ideality factor (n) as seen at the highest intensities shown in Fig. 2. The numerator of k_2 in Eq. (7b) depends on both recombination mechanisms that give $n = 1$: the QNR and the interface recombination. The ratio of the numerator to the denominator (SCR recombination) determines how large a G_{avg} is needed to give unity ideality factor. In this $k_2 G_{avg} \gg 1$ regime, V_{OC} can be written as

$$V_{OC} = 2\frac{kT}{q}\ln[k_1\sqrt{k_2 G_{avg}}] = \frac{kT}{q}\ln\left[\frac{W G_{avg}}{R_0^I + R_0^b}\right], \qquad (11)$$

where the cancellation of R_0^d term in k_1 and k_2 makes V_{OC} independent of SCR recombination. The different temperature dependences of R_0^I and R_0^b then allow the separation of interface and QNR recombination using Eq. (11). Near room temperature (T_R), $V_{OC}(T)$ is normally observed to be linear.[4] Therefore, a characteristic energy, E_a, can be obtained by extrapolating $V_{OC}(T)$ to 0 K through the expression

$$V_{OC}(T_R) = \frac{E_a}{q} + T_R\frac{dV_{OC}}{dT}\bigg|_{T_R}. \qquad (12)$$

The characteristic energy (E_a) is an activation energy associated with an effective energy gap across which carriers recombine;[3] by extrapolating V_{OC} to 0 K, we obtain the maximum possible QFL separation achievable, when there are no thermally generated electron-hole pairs. For band-to-band or defect recombination in the bulk of the semiconductor, $E_a = E_g$. For recombination across interface states,[3] $E_a = \phi^n_{b,0}$. When both recombination mechanisms are active with comparable strengths, E_a takes on a value between $\phi^n_{b,0}$ and E_g. To derive an analytical formula for E_a, we
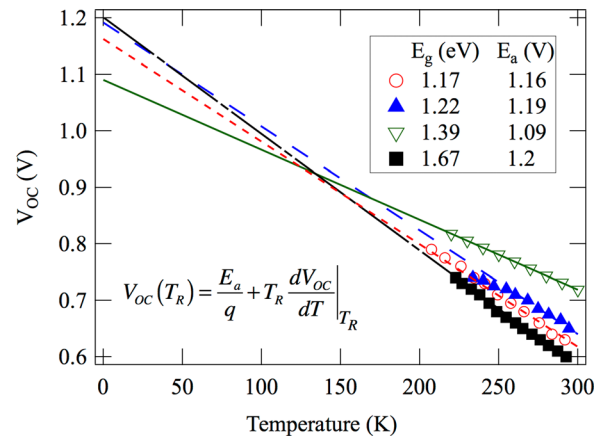

FIG. 3. Open-circuit voltage vs. temperature [$V_{OC}(T)$] for a series of CIGS solar cells with varying bandgap.

substitute the temperature derivative of Eq. (11) expression for V_{OC} into Eq. (12) and obtain

$$E_a = \frac{R_0^b E_g(T_R) + R_0^I \phi^n_{b,0}(T_R)}{R_0^b + R_0^I}. \qquad (13)$$

Thus, E_a is the mean of E_g and $\phi^n_{b,0}$ weighted by the strength of recombination in the bulk and at the interface, respectively.

We apply Eq. (13) to investigate recombination in a series of $Cu(In_{1-x}Ga_x)Se_2$ solar cells, where the bandgap of the absorber is varied by changing the Ga content.[13] From the light intensity dependence of V_{OC}, we confirm that n approaches unity at 1-sun light intensity. Therefore, the light-bias applied is sufficient to satisfy $k_2 G_{avg} \gg 1$ and Eq. (13) applies. $V_{OC}(T)$ is plotted in Fig. 3 for four cells with different bandgaps. Despite a large change in the bandgap from 1.17 to 1.67 eV, the extrapolated activation energy (E_a) remains close to 1.1 eV.

In the CIGS devices, we measured for Fig. 3, the 1-sun V_{OC} does not increase proportionally as E_g increases. This behavior is shown in Fig. 4(a). The saturation of V_{OC} despite
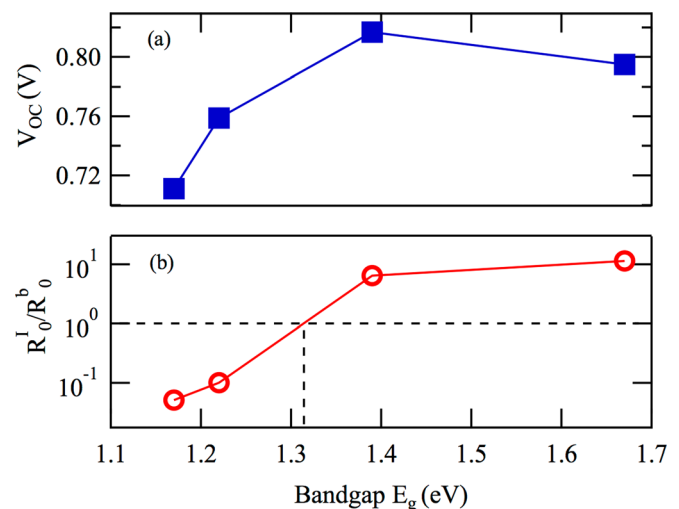

FIG. 4. (a) V_{OC} vs. bandgap (E_g) for CIGS solar cells shown in Fig. 3. The V_{OC} saturates as E_g increases with increasing Ga content. (b) Ratio of interface (R_0^I) and bulk (R_0^b) recombination strengths, calculated using Eq. (13), increases dramatically for the higher bandgap samples.

the increasing E_g has been attributed to increasing interface recombination.[13] However, no quantitative analysis was provided. Using the known values of bandgap and estimating the values of $\phi^n_{b,0}$ from the doping density and the built-in voltage (extracted from C-V measurement), we calculate the ratio R^I_0/R^b_0 from Eq. (13). As shown in Fig. 4(b), the ratio of interface to bulk recombination increases about 2 orders of magnitude with increasing E_g. Below a transition bandgap of about 1.32 eV, $R^I_0/R^b_0 \ll 1$ means that bulk recombination dominates. Above E_g of 1.32 eV, $R^I_0/R^b_0 \gg 1$ means that interface recombination dominates.[14]

The examples treated above demonstrate that our analytically derived dependences of V_{OC} on light-intensity and temperature enable quantitative estimates of the relative strengths of SRH recombination in different regions of the solar cell. The intensity dependence of V_{OC} and the ideality factor are used to differentiate recombination in SCR relative to the QNR and interface contributions. By extrapolating the temperature dependence of V_{OC}, we are able to compute the activation energy for carrier recombination. This activation energy is the mean of absorber bandgap and interface barrier-height as weighted by recombination strengths for QNR and interface pathways.

The formulae used in this work are derived from broadly applicable approximations of the full solar cell transport equations. The SRH analysis mathematically assumes there is a single trap level near midgap. Some solar cell materials present a multiple defect levels or a continuous distribution of defects in the gap. The recombination statistics of a continuous distribution of defects is similar to that of a single defect level near midgap,[15] and an effective cross-section and defect density can be used to analyze recombination in such materials. While we assumed SRH recombination is the dominant recombination mechanism, our framework could also provide the explicit dependence of V_{OC} on other recombination mechanisms.

We do not assume exponential $J(V)$ characteristics nor do we apply the superposition of dark and light $J(V)$ curves, which broadens the applicability of our analysis. Even though the derivations shown above are for an n-type absorber and a type-I heterojunction, the general formulae are applicable to other structures as well. We believe that this approach for experimental determination of recombination in different regions of a solar cell is extremely valuable in diagnosing and improving solar cells, especially those with heterojunction emitters.

[1]M. A. Green, *Solar Cells: Operating Principles, Technology and System Applications* (The University of New South Wales, Kensington, 1998).
[2]S. M. Sze and K. N. Kwok, *Physics of Semiconductor Devices*, 3rd ed. (John Wiley & Sons, Hoboken, NJ, 2007).
[3]R. Scheer, J. Appl. Phys. **105**, 104505 (2009).
[4]S. S. Hegedus and W. N. Shararman, Prog. Photovoltaics **12**, 155 (2004).
[5]K.-I. Ishibashi, Y. Kimura, and M. Niwano, J. Appl. Phys. **103**, 094507 (2008).
[6]W. Shockley and H. J. Queisser, J. Appl. Phys. **32**, 510 (1961)
[7]M. Shur, *Physics of Semiconductor Devices* (Prentice-Hall, Englewood Cliffs, 1990).
[8]S. J. Fonash, *Solar Cell Device Physics*, 2nd ed. (Academic Press, Burlington, 2010).
[9]C. W. Teplin, K. Alberi, M. Shub, C. Beall, I. T. Martin, M. J. Romero, D. L. Young, R. C. Reedy, P. Stradins, and H. M. Branz, Appl. Phys. Lett. **96**, 201901 (2010).
[10]K. Alberi, H. M. Branz, H. Guthrey, M. J. Romero, I. T. Martin, C. W. Teplin, P. Stradins, and D. L. Young, Appl. Phys. Lett. **101**, 123510 (2012).
[11]R. A. Sinton and A. Cuevas, in *Proceedings of the 16th EPVSEC* (Glasgow, 2000), pp. 1152–1155.
[12]S. Grover, C. W. Teplin, J. V. Li, D. C. Bobela, J. Bornstein, P. Schroeter, S. Johnston, H. Guthrey, P. Stradins, H. M. Branz, and D. L. Young, IEEE J. Photovoltaics **3**, 230 (2013).
[13]M. A. Contreras, L. M. Mansfield, B. Egaas, J. Li, M. Romero, R. Noufi, E. R. Voigt, and W. Mannstadt, Prog. Photovoltaics **20**, 843–850 (2012).
[14]Increasing recombination near the CdS/CIGS interface with increasing Ga-composition has been attributed to the higher CIGS conduction band that occurs due to the isovalent Ga-In alloying. Refer to: M. Turcu, I. M. Kötschau, and U. Rau, J. Appl. Phys. **91**, 1391 (2002).
[15]J. G. Simmons and G. W. Taylor, Phys. Rev. B **4**(2), 502–511 (1971).